

# Study on Path Optimization and Motion Prediction for Dragon Dance Based on Helical Models

Yanyang Li<sup>#</sup>, Yibing Shi<sup>#</sup>, Zihan Wang<sup>\*,#</sup>

Information Science and Technology College, Dalian Maritime University, Dalian, China, 116026

\* Corresponding author: wangzi2438816550@dlmu.edu.cn

<sup>#</sup>These authors contributed equally.

**Abstract.** This paper presents a specialized motion prediction model for the complex, coordinated movements characteristic of dragon dance performance, aiming to enhance fluidity and aesthetic appeal through accurate motion forecasting. The model employs a multi-objective optimization approach, utilizing the Salp Swarm Algorithm (SSA) to effectively capture and predict intricate movement sequences. Through detailed analysis of temporal and spatial parameters inherent in dragon dance, the model can address the challenges posed by the dance's dynamic and collective motion requirements. Experimental results verify the model's predictive accuracy and adaptability, showing a significant improvement in forecast precision over traditional methods. These findings highlight the model's capability to handle complex motion interactions, thereby contributing to research in both motion prediction and performance modeling. Furthermore, this approach offers broader applicability, as the insights gained here may benefit various domains where accurate, real-time movement prediction is essential, including robotics, sports analysis, and animation.

**Keywords:** Motion Prediction, Multi-objective, SSA, Dragon Dance.

## 1. Introduction

Bench dragon is a traditional folklore activity born in southern China, which is mainly prevalent in Fujian, Zhejiang, and other regions, and is usually held on festivals such as the Lunar New Year and the Lantern Festival to pray for good weather, good harvests, and national peace [1]. The dragon dance movement of this Chinese art of dragon rhyme involves connecting the heads and tails of multiple decorated benches, with the dragons reaching dozens or even hundreds of meters in length. Since the dragon dance process involves the precise cooperation and control of multiple participants, the optimization of its movement path, speed, and position parameters becomes the key to enhancing the spectacle and safety of the dragon dance performance.

In recent years, along with the development of mathematical modeling and optimization algorithms, researchers have devoted themselves to optimizing the key parameters in dragon dance movement through mathematical models to more effectively design dragon dance performance paths. Archimedes spirals are widely used for path planning, especially for robot navigation and full-area coverage due to their uniform scaling and low energy consumption characteristics [2]. Its polar coordinate equations provide easy-to-calculate trajectories, which are suitable for the design of wrap-around paths for dragon dance movement and can ensure the smoothness and visual effect of the performance. Meanwhile, the superiority of Archimedes' optimization algorithm in path optimization has been verified in spraying robots [3]. Currently, the research on the multi-objective path optimization problem still focuses on the improvement and optimization of group-based methods and those based on Pareto optimal thought [4]. Among the population-based methods, the improved NSGA-II algorithm effectively enhances the convergence speed and accuracy by retaining high-quality individuals and adaptively adjusting the coefficient of variation [5]. The Grey Wolf optimization algorithm (GWO) relies on a dynamic weight adjustment strategy and has strong adaptability [6]. The improved ant colony algorithm improves its comprehensive performance by differentiating the initial pheromone distribution [7]. The improved multi-objective particle swarm optimization algorithm proposed by Feng et al. takes into account both global search and local search by introducing an adaptive Angle partitioning strategy [8]. The Sparrow search algorithm proposed

by Xue et al. in 2020 has the advantages of a simple structure, few control parameters, and strong local search ability [9]. And Mu et al. improved the traditional SSA by introducing strategies such as even symmetric infinite folding chaotic sequences, thereby improving the global search ability and convergence speed of the algorithm [10]. Among the methods based on Pareto optimal thought, the Ripples diffusion algorithm (RSA) generates a complete Pareto frontier solution set, which is also applicable to the global optimization requirements of multi-objective scenes in dragon dance performances [11].

However, in the current optimization of the dragon dance movement path, the dynamic changes of the complex head-turning process are difficult to accurately adapt, resulting in discontinuous trajectories and affecting the coordination of the performance. In addition, the multi-objective optimization algorithm is insufficiently adaptable under the real-time and high dynamic requirements of dragon dance movement, and the accuracy and efficiency of collision detection also need to be improved. To cope with these problems, our study introduces an Archimedean solenoidal geometric model to reduce the length of the turnaround path by improving the geometric properties of the model: fixing the radius, and adopting a centrosymmetric structure. For the multi-objective optimization of path occupancy area and collision risk, we design a dynamic adaptive optimization algorithm based on the sparrow search algorithm, which significantly improves the real-time adjustment capability and safety of the path.

## 2. Movement Model of Dragon Dance

The dragon dance team consists of  $N$  sections of benches, of which the first section is the dragon head and the next  $N-1$  sections are the dragon body. It is noteworthy that the board length of the dragon's head is different from that of the dragon's body, and the benches are connected by handles. Figure 1 shows a front view of the bench.

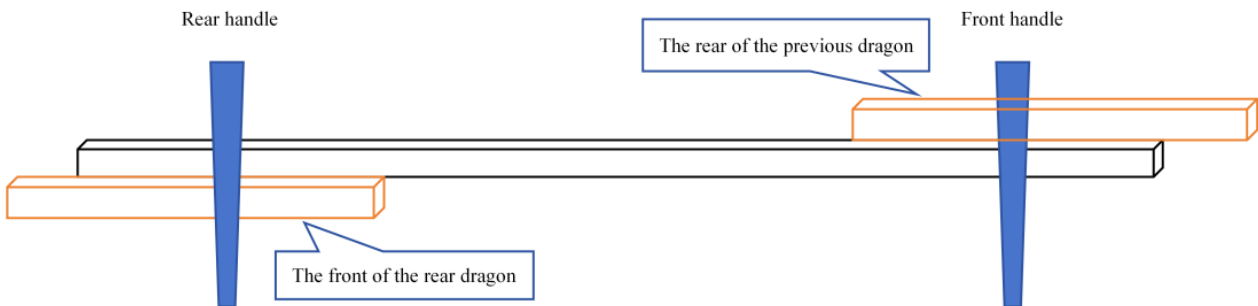


Figure 1. Bench view

### 2.1. Spiral ingress model

#### 2.1.1. The establishment of a spiral equation

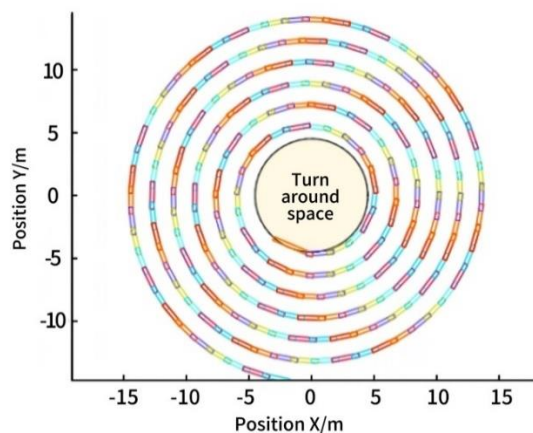
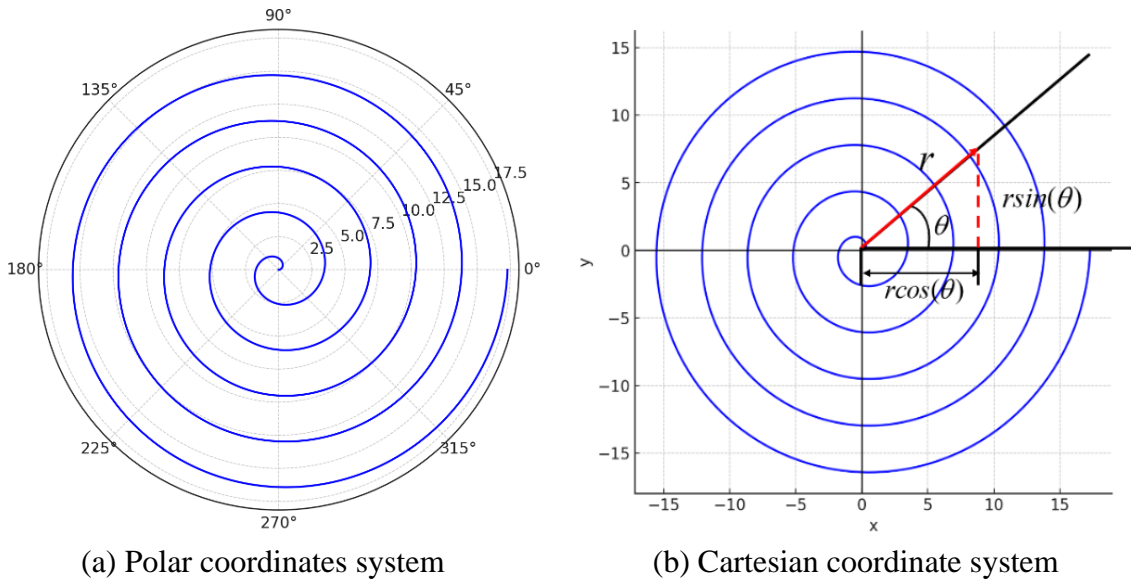


Figure 2. The spiral ingress of the Dragon Dance team

The coiled-in path of the bench dragon is regarded as an Archimedean solenoid, from which a coordinate system is established and the solenoid equation is solved as in Eq.1. Figure 2 shows the schematic diagram of the bench dragon, and Figure 3 shows the solenoidal diagram in the plane right-angle coordinate system and polar coordinate system.

$$\begin{cases} x = r \cos(\theta) = (a + b\theta) \cos(\theta) \\ y = r \sin(\theta) = (a + b\theta) \sin(\theta) \end{cases} \quad (1)$$

Where  $a$  is the initial radius of the screw thread, and  $b$  is the pitch (the increase corresponding to a unit angle), determined by the relationship between pitch and angle change.



**Figure 3.** Helical Diagram

In the Cartesian coordinate system, the limit of derivation for a segment of the arc of the Archimedean solenoid, which can be approximated as a straight line, is given:

$$ds = \sqrt{dx^2 + dy^2} = b\sqrt{1 + \theta^2} d\theta \quad (2)$$

This formula  $dx^2$ 、 $dy^2$  is satisfied:

$$\begin{cases} dx^2 = (r' \cos \theta - r \sin \theta)^2 d\theta = (r'^2 \cos^2 \theta - 2r'r \cos \theta \sin \theta + r^2 \sin^2 \theta) d\theta^2 \\ dy^2 = (r' \sin \theta + r \cos \theta)^2 d\theta = (r'^2 \sin^2 \theta + 2r'r \cos \theta \sin \theta + r^2 \cos^2 \theta) d\theta^2 \end{cases} \quad (3)$$

### 2.1.2. Movement of Dragon Head

Set the angular displacement of the starting point of the faucet as  $\theta_s$ , and the arc length of its passage at any moment as in Equation 4, where  $v_{head}$  is the velocity of the faucet, and  $\theta(t)$  is the corresponding polar angle of the faucet at the time of  $t$ . The position coordinates of the faucet at any moment are shown in Equation 5.

$$S = \int_{\theta(t)}^{\theta_s} b\sqrt{1 + \theta^2} d\theta = v_{head} t \quad (4)$$

$$\begin{cases} x = b\theta(t) \cos[\theta(t)] \\ y = b\theta(t) \sin[\theta(t)] \end{cases} \quad (5)$$

### 2.1.3. Movement of Dragon Body

#### (1) Position

At any moment, the triangle formed by the dragon's head, the front handle of the first section of the dragon's body, and the origin always satisfies the cosine theorem (Equation 6). Let the

corresponding polar diameter corresponding to the  $i$ th section of the dragon's body (i.e., the distance from the origin to the front handle of the dragon's body in section  $i$ ) be  $l_i$ , the corresponding polar angle be  $\theta_i$ , and the centroid distance between the two handles of the dragon's body be known and noted as  $L_{body}$ . Then, using the cosine theorem, it is concluded that the front handle of the dragon body in section  $i$  and the front handle of the dragon body in section  $i-1$  at any moment satisfy Equation 7.

$$(b\theta_0)^2 + (b\theta_1)^2 - L_{head}^2 = 2b^2\theta_0\theta_1\cos(\theta_1 - \theta_0) \tag{6}$$

$$l_i^2 + l_{i-1}^2 - L_{body}^2 = 2l_i l_{i-1} \cos(\theta_i - \theta_{i-1}) \tag{7}$$

In Eq. 6,  $\theta_0$ ,  $\theta_1$  is the polar angle corresponding to the front handles of the dragon head and the first section of the dragon body, respectively, and  $L_{head}$  is the centroid distance between the two handles of the dragon head.

(2) Speed

In the triangle formed by the front and rear handles of the dragon body of section  $i$  and the origin, let the angle between the front handle and the dragon body be  $\alpha_{i-1}$ , and the angle between the rear handle and the dragon body be  $\beta_i$  as shown in Figure 4. Let the coordinates of point C be  $(x_i, y_i)$  and the coordinates of point B be  $(x_{i-1}, y_{i-1})$ . The velocity direction of each handle is tangent to the solenoid, then for any point on the solenoid, the unit vector in the direction of its velocity can be expressed as  $(1, \frac{dy}{dx})$ , the bench is considered as a rigid body, then the  $i-1$  section of the dragon body and the  $i$  section of the dragon body of the front handle along the direction of the bench has the same velocity component, according to this can be obtained from the adjacent two handles between the speed of the relationship is as follows:

$$v_{i-1} \cos \alpha_{i-1} = v_i \cos \beta_i \tag{8}$$

This can be further obtained by substituting the unit vectors in each velocity direction into the expression at  $v_i$  based on the vector triangles in Figure 4:

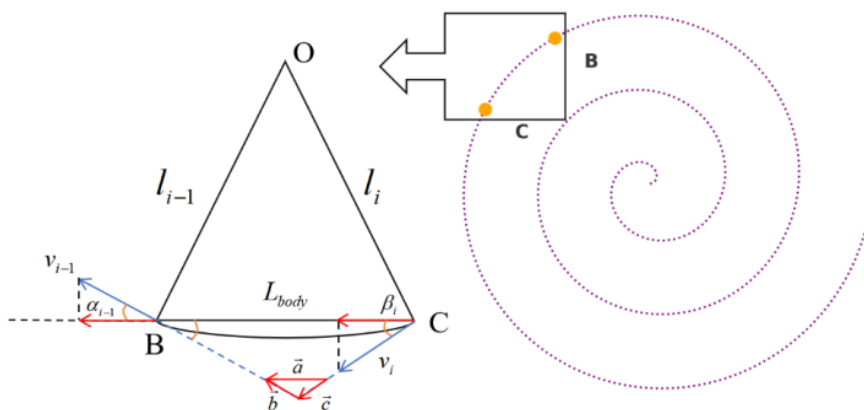


Figure 4. Geometric relationship of adjacent handles

$$v_i = \frac{|\vec{a}\vec{b}|}{|\vec{a}\vec{c}|} v_{i-1} \tag{9}$$

Where  $\vec{a}$  is the unit vector in the  $\overline{CB}$  direction,  $\vec{b}$  represents the unit vector in the direction of the velocity at point C, and  $\vec{c}$  means the unit vector in the direction of the velocity at point C.

### 2.2. Turning model

Our model adopts a fixed radius and a centrosymmetric structure to optimize the turnaround path of the dragon dance team, i.e., the coil-out and coil-in solenoids are centrosymmetric about the center of the solenoids. The dragon dance team completes the turnaround in the set turnaround space, and the turnaround path is an S-shaped curve connected by the tangency of two arcs, the radius of the first arc is twice that of the latter, which is tangent to both the disk-in and disk-out solenoids. The turnaround path is shown in Figure 5.

Assuming that the motion of the faucet has been computed by the solenoidal equations and that the position of each handle of the faucet (front and back) is known, let the two neighboring sections of the bench be section and section, whose distances are kept constant, and whose lengths are (the lengths of the given benches). Then the coordinates of the section are computed from the coordinates of the section through a fixed pole shift direction:

$$\begin{cases} x_{i+1}(t) = x_i(t) - L_i \cos(\theta_i(t)) \\ y_{i+1}(t) = y_i(t) - L_i \sin(\theta_i(t)) \end{cases} \quad (10)$$

The velocity of each bench section is the rate of change of its displacement with respect to the previous section with respect to time, which can be approximated by the difference method.

$$\begin{cases} v_x^{(i+1)}(t) = \frac{x_{i+1}(t) - x_{i+1}(t-1)}{\Delta t} \\ v_y^{(i+1)}(t) = \frac{y_{i+1}(t) - y_{i+1}(t-1)}{\Delta t} \end{cases} \quad (11)$$

Where  $\Delta t$  is the time step (1 second).

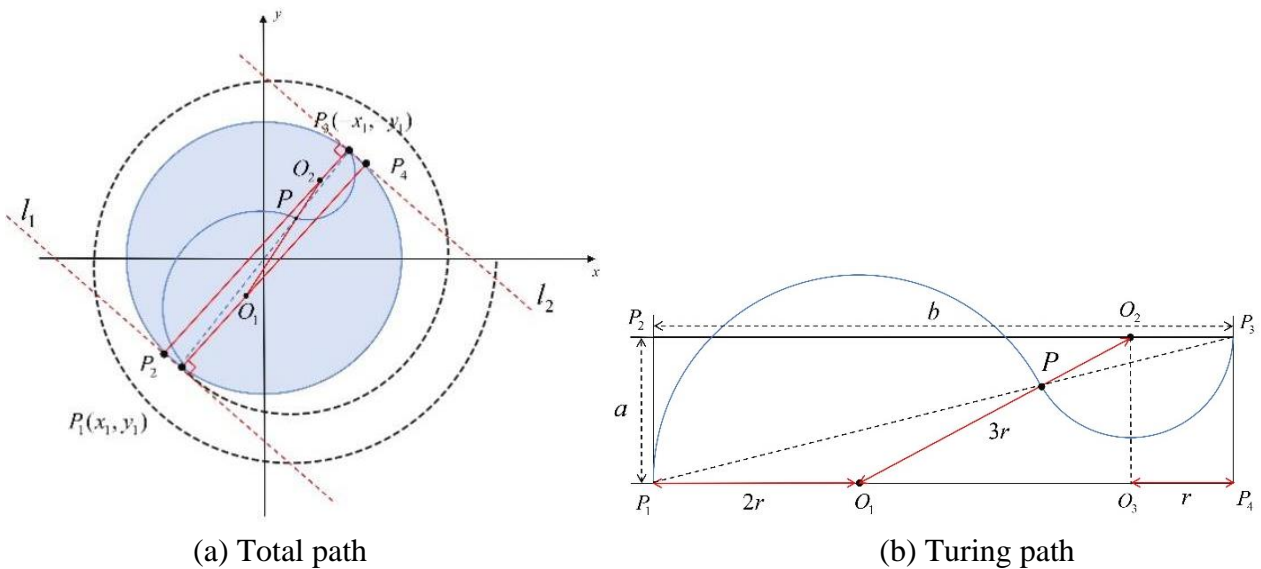


Figure 5. Turing path diagram

### 2.3. Multi-objective optimization model

The movement of the Dragon Dance Team includes three processes: traveling into  $P_1$  point, turning around, and traveling out from  $P_3$  point. Generally speaking, under the premise that the dragon dance team can coil in and out freely, the smaller the area needed to coil the dragon, and the faster the traveling speed is, the better the spectacle is. Based on this, we propose a multi-objective optimization model to seek the dragon's head speed at optimal spectacle. The objective function is as follows:

➤ **Minimize footprint**  $f_1$

The smaller the area required to coil the dragon, the better the spectacle. This can be expressed by the area of the convex envelope formed by the dragon dance team in each time step  $A(t)$  :

$$\min f_1 = \int_0^T A(t)dt \tag{12}$$

➤ **Minimize collision risk**  $f_2$

To ensure smoothness and safety when coiling the dragon, the minimization of collision risk needs to be considered in the optimization. Defining the distance between non-adjacent dragon body segments  $d_{i,j}(t)$ , the objective function of collision risk can be expressed as:

$$\min f_2 = \sum_{i,j} \max(0, d_{safe} - d_{i,j}(t)) \tag{13}$$

Where  $d_{safe}$  is the set safe distance between non-adjacent benches.

The constraints are as follows:

$$s.t. \begin{cases} d_{i,i+1}(t) = L \\ v_i(t) \leq v_{max} = 2m / s \\ d_{i,j}(t) \geq d_{safe}, i \neq j \end{cases} \tag{14}$$

Where  $v_i$  is the bench speed per section and  $d_{i,j}$  is the distance between the two benches.

### 3. Results

#### 3.1. Spiral ingress result

In the second part of this study, we modeled the motion of the faucet's disk-in and disk-out. The simulated data were based on an isometric spiral with a pitch of 1.7 m, while the head-turning path was designed as an S-shaped curve consisting of two tangent circular arcs, where the radius of the front arc was twice as much as that of the back one, ensuring smooth tangency with the coil-in and coil-out spirals. Specific to the physical parameters of the dragon dance team, the board length of the dragon head section is 341 centimeters, while the board lengths of the dragon body and tail are both 220 centimeters, and the board width of all the benches is 30 centimeters. In addition, each bench section is equipped with two holes of 5.5 cm in diameter, the centers of which are 27.5 cm from the respective board heads.

Through data simulation techniques and precise code implementation, we were able to simulate the movement trajectory of the dragon dance team second by second. In this process, we first calculated the position of the front handle of the dragon's head, and then based on the precise geometrical relationship between the dragon's head and the dragon's body, as well as between the sections of the dragon's body, we sequentially deduced the position of each section of the dragon's body. At the same time, with the help of the relationship equation between the previous section of the dragon body and the current speed of the dragon body derived in the model, we were able to calculate the speed of each section of the dragon body in each second. The results of these calculations, including the positional coordinates of each point and the magnitude of the velocity, are recorded in detail in Tables.1. and 2. The 0th second is the head-turning moment, when the position of the front handle of the dragon head reaches the position of the innermost circle at the head-turning moment, and the position of the dragon body sections reaches the tightest alignment at the head-turning moment.

**Table 1.** Positions of each point

|                  | -100s      | -50s      | 0s        | 50s      | 100s      |
|------------------|------------|-----------|-----------|----------|-----------|
| Faucet x(m)      | 5.70459    | 2.133281  | 0.811531  | 1.685673 | 5.691689  |
| Tap y(m)         | -5.071049  | -5.18786  | 0.770517  | 5.654954 | 5.291213  |
| Section 1 x(m)   | 6.431789   | 0.869821  | 3.586853  | 4.706859 | -3.252324 |
| Section 1 y(m)   | -3.374446  | -6.201285 | -0.01938  | 2.392245 | 6.483596  |
| Section 51 x(m)  | -6.22823   | 8.849536  | 5.706692  | 0.304377 | 3.383425  |
| Section 51 y(m)  | 6.540798   | -3.120956 | -3.523193 | 4.537491 | -0.222038 |
| Section 101 x(m) | -12.770539 | 6.701455  | 7.729718  | 1.457933 | 3.726244  |
| Section 101 y(m) | 5.70459    | -2.133281 | 0.811531  | 1.685673 | -5.691689 |
| Section 151 x(m) | -5.071049  | -5.18786  | 0.770537  | 5.654954 | 5.291213  |
| Section 151 y(m) | 6.431789   | 0.869821  | 3.586853  | 4.706859 | -3.252324 |
| Section 201 x(m) | -3.374446  | -6.201285 | -0.01938  | 2.392245 | 6.483596  |
| Section 201 y(m) | -6.22823   | -3.120956 | -3.523193 | 4.537491 | -0.222038 |
| Tail(rear) x(m)  | 6.540798   | -3.120956 | -3.523193 | 4.537491 | -0.222038 |
| Tail(rear) y(m)  | -12.770539 | 6.701455  | 7.729718  | 1.457933 | 3.726244  |

**Table 2.** Speed at each point and time

|                     | -100s    | -50s     | 0s       | 50s      | 100s     |
|---------------------|----------|----------|----------|----------|----------|
| Faucet (m/s)        | 1        | 1        | 1        | 1        | 1        |
| Section 1 (m/s)     | 1.006824 | 1.006811 | 1.006796 | 0.993149 | 0.993273 |
| Section 51 (m/s)    | 1.006857 | 1.006843 | 1.006822 | 0.993002 | 0.993128 |
| Section 101 (m/s)   | 1.006914 | 1.006895 | 1.006849 | 0.992901 | 0.993108 |
| Section 151 (m/s)   | 1.006983 | 1.006921 | 1.006903 | 0.992831 | 0.993011 |
| Section 201 (m/s)   | 1.007038 | 1.007033 | 1.006988 | 0.992865 | 0.993042 |
| Dragon's tail (m/s) | 1.007147 | 1.007092 | 1.007016 | 0.992742 | 0.993081 |

(1) Position analysis

The size of the pitch directly affects the tightness and space required when the dragon dance team is coiled in. As the dragon dance team moves into the inner circle along the spiral line, the space taken up gradually increases. The width (30 cm) and length (220 cm) of the benches determine the floor space of each section of the dragon body when coiling in, which is essential to avoid collisions between benches and ensure smooth movement.

The dragon's head serves as a guide for the dragon dance team, and its position changes according to the pitch and time. During the coiling-in process, the dragon head moves along the spiral to the inner circle, and its position can be determined by converting polar coordinate equations to right-angle coordinate equations. Through simulation, we calculated the position of the front handle of the dragon head. The position of each section of the dragon's body depends on the position of the dragon's head and the previous section of the dragon's body. Through geometric relationships and the cosine theorem, we can calculate the position of each dragon body section recursively. Due to the constant pitch, the position of the dragon's body shows a regular variation.

(2) Velocity analysis

The speed of the dragon's head is constant at 1 m/s, which is the base speed for the dragon dance team to coil in and out. Calculation of the dragon's body speed shows that it decreases over time. In the process of coiling in, the radius of curvature of each section of the dragon's body decreases as the dragon's head moves along the spiral to the inner circle. According to the law of circular motion, the velocity of an object on a circular path is inversely proportional to its distance to the center of the circle (i.e., the radius of curvature). Therefore, as the radius decreases, the velocity of each section of the dragon's body decreases accordingly to keep the angular velocity constant.

(3) Proof of uniqueness

In the following, we prove the uniqueness of the turnaround path. To facilitate the proof, we set the pitch of the disk-entry solenoid as 1.7 m, and the radius of the turnaround space as 4.5 m. The

coordinates of the starting point and the ending point of the turnaround, when the faucet travels along the disk-entry solenoid to the boundary, are  $P_1(-2.711856, -3.591078)$ ,  $P_3(2.711856, 3.591078)$  respectively. The slopes of the two tangent lines  $l_1, l_2$  can be calculated from the solenoidal derivatives. Knowing the slope and the point on the line, the expressions for the two tangent lines are  $l_1: y = -1.504093x - 7.669962$  and  $l_2: y = -1.504093x + 7.669962$  respectively. Therefore, the distance between the two tangents, i.e., the length of the rectangle  $b = 8.493008$  in Figure 5(b). And there is  $P_1P_3 = 9.0$  m, according to the Pythagorean theorem to find the width of the rectangle  $a = 2.978056$  m. The line segment  $O_1O_2$  and the intersection of the path of the turnaround  $P$  is exactly the point where the two segments of the arc meet, according to the geometric relationship in Figure 5(b), which can be found P-point coordinates of  $P(-1/3x_1, -1/3y_1) = (0.903952, 1.197026)$ . The triangle  $O_1O_2O_3$  satisfies the Pythagorean theorem, then the radius of the small circle  $r = 1.589543$  m.

And because  $O_1$  lies on the line  $P_1P_4$  (slope  $k_{P_1P_4} = -1/k = 0.664853$ ), then:

$$(x_{O_1} - x_1)^2 + (y_{O_1} - y_1)^2 = (2r)^2 \quad (15)$$

$$\frac{y_{O_1} - y_1}{x_{O_1} - x_1} = 0.664853 \quad (16)$$

Join Eq.10 and Eq.11 to find  $O_1(-0.06448, -1.830972)$ , and the same can be done for  $O_2(1.388169, 2.711018)$ .

So far, we find that the centers of the two arc segments of the turnaround path are fixed points and the radii are fixed values, i.e., the turnaround path is fixed.

### 3.2. Dynamic Adaptive Optimization Algorithm

---

#### Algorithm Sparrow Search Algorithm SSA

---

- 1: Inputs:  $n$  (population size),  $PD$  (number of finders)  $SD$  (number of vigilantes),  $R_2$  (warning value),  $T$  (maximum number of iterations), and the initial position of the sparrow population;
  - 2: Output:  $X_{best}$  (optimal sparrow position),  $f_{best}$  (optimal fitness value)
  - 3: **while** ( $t < T$ )
  - 4: Sort the current fitness values to find the location of the optimal and the worst individuals.;
  - 5:  $R_2 = rand(1)$
  - 6: **for**  $i = 1 : PD$
  - 7: Update the finder's position;
  - 8: **end**
  - 9: **for**  $i = (PD + 1) : n$
  - 10: Update follower positions;
  - 11: **end**
  - 12: **for**  $i = 1 : SD$
  - 13: Updating the position of the vigilante;
  - 14: **end**
  - 15: Update the current optimal individual position;
  - 16:  $t = t + 1$
  - 17: **end while**
  - 18: **return**  $X_{best}, f_{best}$
-

In this paper, the Improved Sparrow search algorithm (SSA) proposed by Chen et al was adopted to solve the multi-objective optimization model [12]. Compared with other optimization algorithms such as NSGA-II and GWO, the SSA we used showed obvious advantages in the following aspects: the SSA optimizes by imitating the sparrow's foraging behavior, with a strong global search capability, which can avoid falling into the local optimum effectively, and thus find a solution closer to the global optimum in the complex multi-objective optimization; it has a faster convergence speed; it can dynamically adjust the search strategy according to the changes in the environment, which makes it more flexible and effective when dealing with dynamic path planning; it is simple in structure and easy to implement, which is suitable for the multi-objective optimization. find a solution closer to the global optimum; it has a faster convergence speed; it can dynamically adjust the search strategy according to the changes in the environment, which makes it more flexible and effective in dealing with dynamic path planning problems; it has a simple structure, is easy to implement, and applies to a wide range of optimization problems, including multi-objective optimization of path occupancy area and collision risk.

The pseudo-code of the sparrow search algorithm SSA is given to represent the specific process of SSA more intuitively. After solving, the maximum traveling speed of the dragon head is 1.878 m/s. In the analysis of the speed of all parts of the dragon body and the dragon tail, the speed of the whole dragon dance team is in a small range of space, and to ensure that the maximum value of the speed of the dragon body is less than 2 m/s, to be able to ensure the stability of the overall team, and be able to smoothly complete the spiral circling.

#### 4. Conclusion

In this study, we carried out an in-depth analysis and solution for the parameter optimization problem in the dragon dance movement using mathematical modeling and numerical simulation. The results show that the turning path of the dragon dance team is unique through strict mathematical verification. By accurately calculating the position and speed of the dragon dance team, our model enables the performers to better control the dragon dance formation, avoid collision, and improve the smoothness and spectacle of the performance. In addition, the model can be used to analyze how to optimize the traveling path of the dragon dance team when the size of the bench, the turnaround area, or the shape of the circling path changes, allowing us to achieve more efficient performances in limited space, which is especially important for space-constrained occasions such as urban festival celebrations. Another promotion direction is to apply it to robot path planning, intelligent transportation systems, fleet scheduling, and other fields.

#### References

- [1] Wei Huali. The Status quo and inheritance of Benlong Culture in Beiquan [D]. Southwest University, 2012.
- [2] Wang Dong, Zhou Kepu. Full area coverage path Planning based on Archimedes Spiral Travel Method [J]. Industrial Control Computer, 2018, 31 (05): 83 - 84+87.
- [3] Wang Jingxi, Li Yi, Zhang Cheng. Spraying robot path optimization based on Archimedes algorithm [J]. Automation and instrumentation, 2024, (5): 191 - 194 + 199.
- [4] Wang Ziqiang, Hu Xiaoguang, Li Xiaoxiao, et al. Overview of global path planning algorithms for Mobile Robots [J]. Computer Science, 2019, 48 (10): 19 - 29.
- [5] Bao Xianzhe, Song ANI. Improved NSGA-II Algorithm for Vehicle Routing Optimization in Multi-objective Logistics [J]. Computer Applications and Software, 2023, 40 (02): 274 - 280.
- [6] Wang Hongchao. Research on vehicle routing optimization of fresh product cold chain logistics considering dynamic demand [D]. Henan agricultural university, 2024.

- [7] Wang Fengsheng, Du Li, Xu Guanghui. Based on improved ant colony algorithm in the distributed multi-robot cooperative path planning [J]. Journal of south-central university for nationalities (natural science edition), 2023, and (5): 650 - 657.
- [8] Feng Qian. Multi-objective optimization based on improved particle swarm algorithm and its application [D]. Beijing university of science and technology, 2022.
- [9] Xue Jiankai. A new group of the research and application of intelligent optimization technology [D]. Donghua university, 2020.
- [10] Mou Yuanming, Zhuo Ran, Gao Fei. Path planning of Agricultural Mobile Robot based on Hybrid improved Sparrow Search Algorithm [J]. Chinese Journal of Agricultural Mechanization, 2024, 45 (09): 234 - 243.
- [11] Hu Xiaobing, Chen Shunian, Zhang Yingfei, et al. Ripple Diffusion Algorithm for Multi-objective path Optimization [J]. Computer Engineering and Applications, 2021, 57 (23): 81 - 90.
- [12] Chen Jiajun. The sparrow search algorithm based on improved intelligent vehicle path planning research [D]. Taiyuan university of science and technology, 2023.